Rough Surface Description System in 2,5D Map For Mobile Robot Navigation

Submitted: 26th December 2012; accepted: 17th May 2013

Adam Niewola

Abstract:
This paper presents a new solution in the roughness description based on 2,5D map. Three parameters for rough surface description were proposed. The research was performed to verify which parameter provides the best combination of time calculation and accuracy of the terrain roughness reconstruction. Prepared map may be used for mobile robot path planning.

Keywords: *mobile robot, navigation, 2,5D map*

1. Introduction

Mobile robots are used in wide range of tasks. Robots which deserve a particular attention are these ones which operate in the rough terrain, for example exploration robots or robots used by army.

The mobile robots navigation problem involves several aspects. The localization is to find the position and orientation of the robot in the workspace in relation to the map of the robot [15]. The path planning includes finding the optimal path from the start to the goal position in relation to applied criteria. The next step, robot follows generated trajectory and collects the information about the environment which is used to update the map.

The map of the environment has a big impact on the accuracy of reaching the goal position as well as the possibility of passing generated path. The issue of the path planning process is very often considered by the scientists. There are several types of approaches which may be divided into two groups.

Roadmap methods are to create a net of roads where robot may move without any collision. This leads to the creation of graph which afterwards is searched to find an optimal path. Roads net may be created with the use of different methods. In visibility graph method a graph is created by connecting vertices of obstacles. In the Voronoi diagram method roads are created by pointing out the paths whose distances to two neighboring obstacles are equal. Graph vertices are placed in the points where 3 paths connect [9].

The created graph may be searched with the use of different algorithms, e.g. the depth first algorithm, Dijkstra's algorithm and A* algorithm. The last one is very common. Many modifications of this algorithm were performed for implementing it in various applications (e.g. for fast replanning – [6] and [7]).

Another type of path planning methods are potential methods [9]. They used a potential field created with the use of the start and the goal position and the positions and shapes of obstacles. The main problem in these methods are the local minima which exists in potential fields. They prevent the goal position from being achieved. There are several ways of avoiding of the local minima ([10]).

There is a wide range of relatively novel algorithms for path planning, e.g. genetic algorithms, memetic algorithms ([12]) and probabilistic methods ([13] and [14]).

There are several types of maps used for the mobile robots. The most common are the 2D cell maps with the status (free, occupied or unknown) assigned to each cell. This approach cannot be applied for the mobile robots that operate in an open environment with a high roughness level. The cell description as free or occupied is not enough because some obstacles may be overcome with higher energy consumption, some of them may be overcome only in one way (e.g. moving down the hill may be possible in contrast to moving up). Except that there some obstacles occurs, like small water tanks, sandy areas or small plants which robot may also overcome but with limited velocity. The environment like this makes that for the effective path planning there is a need of appropriate terrain description in the workspace map.

Maps commonly used in mobile robots systems may be divided in three groups [1], [2]:

- the occupancy grids – the 2D cell maps (square, rectangular, hexagonal) with status assigned to each cell; the distance between two cells represents real distance between two points,
- the topological maps – the graph structured maps which show connections between the most important elements of the environment; the distance between two elements of the map does not correspond to the distance between them in the real environment,
- the hybrid maps – the topological-metric maps which are built as the system of local occupancy grids which are the graph nodes in the global topological map.

Maps which are used for the mobile robots which operate in rough terrain are most commonly 2,5D maps ([3],[4],[5]). They are an expansion of standard 2D maps. Each cell may store a number of parameters for appropriate terrain description.

There are also some combined approaches. In [11] a 2D map each cell is subdivided in 16×16 2,5D maps with height parameter, roughness parameter and slope parameter. All of these parameters are used to compute the traversability index gathering the information about the ease-of-traverse of the terrain.

In some cases 2,5D map is not enough and then 3D maps are used. They are mainly used when robot operates in 3D environment (e.g. underwater mobile robots or air mobile robots). They are rarely proposed for land mobile robots due to high number of empty cells.

In [15] a new method for 3D map building is proposed. It uses the stereo vision for gathering the information about the terrain height. It does not need the disparity map and that is why it reduces the computation cost and can be used in the real-time systems.

2. Information gathering

In this paper an attempt was made to find a set of parameters describing the rough surface for mobile robot navigation. This paper deals with gathering information by the robot and does not take into account the localization process of mobile robot.

The parameters required for rough surface description from the point of view of path planning are mentioned below:

- the altitude parameter;
- the small roughness description parameter;
- the information confidence parameter.

Research scene was the point cloud of rough surface terrain received from 3D laser scan. The most common laser scanners are:

- the triangulation scanners – provide the information about the distance with the use of the angle of reflection;
- the time reflection scanners – measure the time between stream emission and detection;
- the phase shift scanners – similar to the time reflection scanners; they provide higher accuracy thanks to phase shift measurement.

The measurement error is an integral part of each measurement. In the laser scanners, particularly these scanners which are installed on the mobile robots, the error is caused by inaccurate positioning of the scanner in relation to robot. It is also caused by the errors in the robot localization process [16]. The point coordinates obtained by the scanner in global map coordinates system may be noted:

$$r_{P,0} = T_{0,R} \cdot T_{R,S} \cdot r_{P,S} \tag{1}$$

where: $r_{P,0}$ – the P point position in the base coordinates system, $T_{0,R}$ – the transformation matrix from the base coordinates system to the mobile robot coordinates system, $T_{R,S}$ – the transformation matrix from the robot coordinates system to the scanner coordinates system, $r_{P,S}$ – the P point position in the scanner coordinates system.

Due to errors mentioned above, the point obtained from the scanner is not described by 3 coordinates in base coordinates system but it is a sphere with a range where its coordinates may vary. This may be shown as an ellipsoid where the coordinates of the obtained point may occur with highest probability (Fig. 1).

On the basis of laser scans of the rough surface terrain several tests were performed in order to verify which parameters should be used to describe the mobile robot environment in 2,5D map.

The parameters which were taken into consideration were:

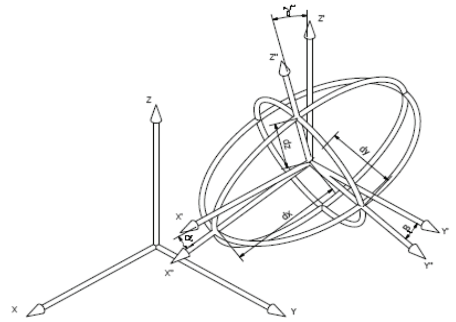

Fig. 1. The error of the point coordinates calculation by the laser scanner

- the parameter describing altitude – average height, maximum height and mean range height (definitions below) from each cell,
- the roughness index – standard deviation and range in each cell,
- the confidence level index – confidence level and confidence factor.

The view of one of the tested areas is shown in the Fig. 2.

Fig. 2. View of tested area

3. The altitude description

The cell altitude was described in 3 ways:

- the average height – equation (2),
- the mean range height – equation (3),
- the maximum height – equation (4).

$$h_{cell} = \frac{1}{n}\sum_{i=1}^{n} h_i \tag{2}$$

$$h_{cell} = h_{min} + \frac{h_{max} - h_{min}}{2} \tag{3}$$

$$h_{cell} = h_{max} \tag{4}$$

where: h_{cell} – cell altitude, h_i – point height, n – number of points in the cell, h_{max} – maximum height of point in the cell, h_{min} – minimum height of point in the cell.

Results of the average height computation depending on the cell dimensions were shown in Fig. 3 as an example. When cell dimensions decrease the precision of description of the environment in the map increases.

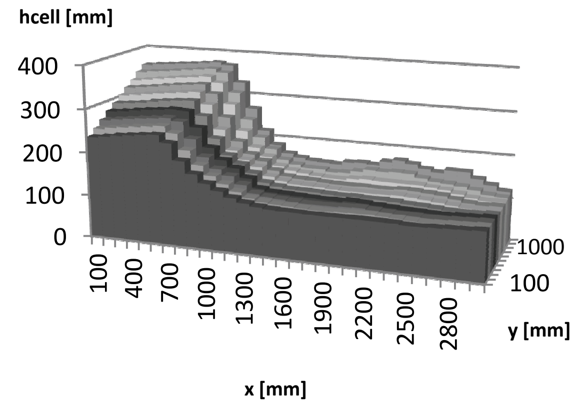

Fig. 3a. Terrain description with the use of average height (cell 100x100 mm)

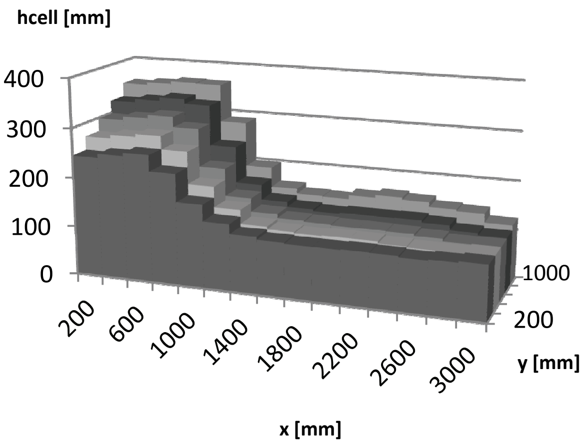

Fig. 3b. Terrain description with the use of average height (cell 200x200 mm)

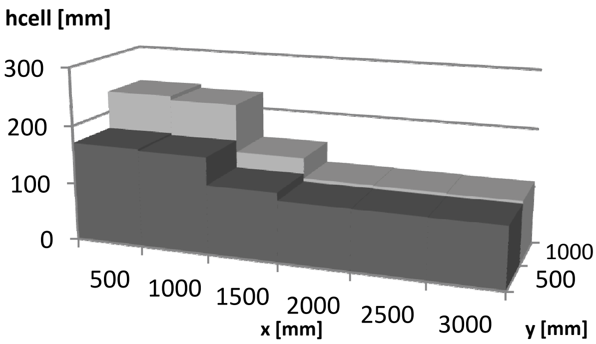

Fig. 3c. Terrain description with the use of average height (cell 500x500 mm)

Fig. 3d. View of tested area

Parameters describing the average height were tested for different cell dimensions. Time calculation for the whole map, as well as one-point-adding to the map, were verified. Two algorithms were implemented in cell heights calculation process for the whole map. First one was to assign each point to its cell, and then to calculate an average value in each cell (dividing and calculating algorithm). The second algorithm was calculating average value point-by-point. Each point was added to its cell and then the average value in the cell was updated (point-by-point updating algorithm).

The map dividing and average height calculating algorithm has the O(n^2) time complexity. The point-by-point calculation algorithm has the O(n) time complexity.

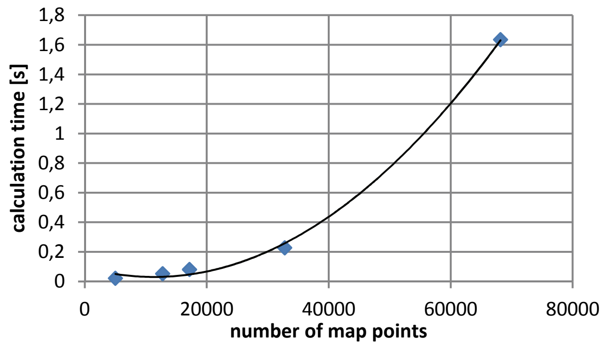

Fig. 4. Average height calculation time for the whole map with 100x100 mm cells with the use of dividing and calculating algorithm

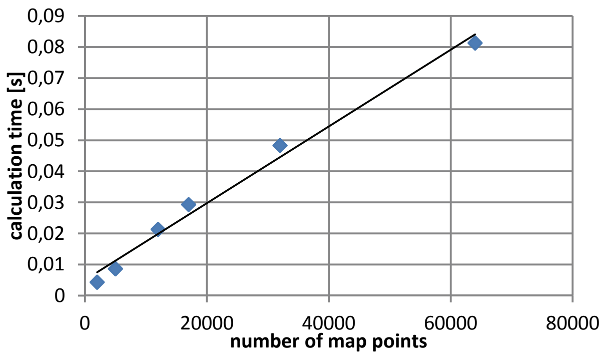

Fig. 5. Average height calculation time for the whole map with 100x100 mm cells with the use of point-by-point updating algorithm

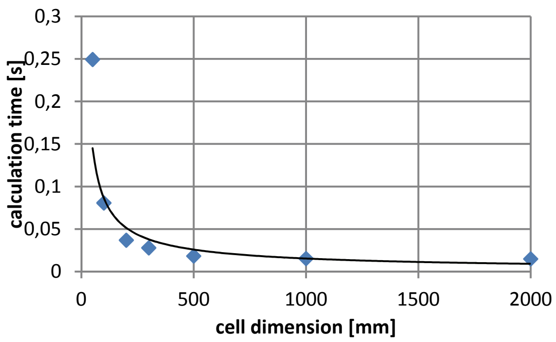

Fig. 6. Average height calculation time for the whole map consisted of ~17000 points with the use of dividing and calculating algorithm

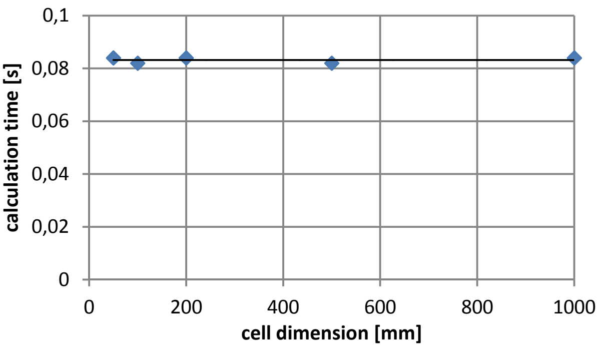

Fig. 7. Average height calculation time for the whole map consisted of ~64000 points with the use of point-by-point updating algorithm

Comparison of these 2 algorithms for the average value calculation was shown in Figs. 4 and 5. It confirms the time complexity of these two methods.

When cell dimensions increase, time calculation decreases while using the first algorithm (Fig. 6). When alternative algorithm was used, time calculation was constant while increasing the cell dimensions (Fig. 7).

Cell dimensions (map granularity) should be combined with the dimensions of the robot. Because of the calculation time, big dimensions of cell are demand. However, due to the precision of the terrain description smaller cells are more suitable (10–30% of the robot width).

In the mobile robots applications more important than calculating the heights for the whole map (map preparation for navigation) may be map updating with the use of the information from the sensors. It takes into consideration adding single points to the map obtained from the laser scanner. Updating the new average value requires the use of the formula:

$$h_{cell\_new} = \frac{h_{cell} \cdot n + h_{new}}{n+1} \tag{5}$$

where: $h_{\mathrm{cell\_new}}$ – updated cell average height value, h_{new} – height value for new point, n – number of points in the cell.

Every time when a new point is obtained by the scanner, average value in one (or more) cells should be updated. Whereas using other cell height parameters (e.g. maximum height or mean range value) cell height value may be updated only when new point has higher value than maximum in the cell or lower than minimum.

Comparison of these three parameters as a cell height value was shown in Tab. 1.

Tab. 1. Cell height value calculation after single point adding

parameter	calculation time for adding of 1000 new points to the map [ms]
average height	0,042
mean range height	0,034
maximum height	0,028

Results of the single point adding allow to sample new points from the terrain with the frequency of MHz. It is more than typical laser scanners (up to 100 kHz) offer. However, results shown in Tab. 1 may be far from single point adding in real mobile robot system due to mobile robot localization time consumption but it is out of scope of this paper. According to the obtained results, calculation time should not be factor which can be used to decide which parameter may be used to describe the rough surface. The average height value was chosen because it provides the best accuracy. In proposed solution terrain slope will be described by the cell heights differences.

4. Roughness Index

The roughness index is the parameter which describes the height differences in each cell. The average height provides the information about the differences in the height of the cells and the roughness index is used to inform the path planner how the terrain height may vary in the cell. The average height smoothes the information about the terrain height and that is why the use of the parameter for roughness is also important. It provides the information about sudden jumps, big slopes and other vertical obstacles (e.g. walls). The roughness index will not need to be used, if the cell dimensions are small enough to provide the information about the vertical obstacles but it is connected with longer computation time.

The roughness may be described as the local difference in the terrain height. Cell height difference may provide good results only when cell dimensions are small enough. In other case there should be a parameter that shows the level of roughness in each cell. This parameter can be:

— the standard deviation of height in each cell:

$$S_{cell} = \sqrt{\frac{\sum_{i=1}^{n}(h_{cell} - h_i)^2}{n-1}} \tag{6}$$

— the height range in each cell:

$$R_{cell} = h_{max} - h_{min} \tag{7}$$

The range calculation time is much shorter and does not require conversion the heights to real type. Evaluation of the new range in the cell after adding new point to the cell is also much faster. Calculating the new standard deviation after adding new point to the map requires the use of the formula:

$$S_{cell\_new} = \left[\frac{1}{n}\left((n-1){S_{cell}}^2 + n{h_{cell}}^2 - (n+1){h_{cell\_new}}^2 + {h_{new}}^2\right)\right]^{0,5} \tag{8}$$

where: S_{cell_new} – new standard deviation, S_{cell} – standard deviation before adding new point, h_{cell} – average height before adding new point, h_{cell_new} – average height after adding the new point, h_{new} – height of new point, n – number of points in the cell (before adding new point).

Comparison of the range and standard deviation calculation was shown in Tab. 2.

Tab. 2. Cell roughness index calculation after single point adding

parameter	calculation time for adding of 1000 new points to the map [ms]
range	0,078
standard deviation	0,030

Results shown in Tab. 2 also allows for sampling the environment with higher frequency than typical laser scanners provides. Because range calculating is much shorter and does not require using real numbers format, this parameter was chosen to describe the roughness in each cell.

5. Confidence Factor

The confidence level of the gathered data may be described using the statistical definition of the confidence level. Because of evaluating the cell height value with average height value, the expected value of height in the cell μ_{cell} may vary with the confidence level 1-α between:

$$h_{cell} - u_{\alpha/2}\frac{S_{cell}}{\sqrt{n}} \le \mu_{cell} \le h_{cell} + u_{\alpha/2}\frac{S_{cell}}{\sqrt{n}} \qquad (9)$$

where $u_{\alpha/2}$ – α/2-quantile of N(0,1) normal distribution.

Assuming the applied value of the permissible variability of μ_{cell} confidence level may be calculated as:

$$1-\alpha = \frac{1}{2\pi}\int_{\frac{-d\sqrt{n}}{2S_{cell}}}^{\frac{d\sqrt{n}}{2S_{cell}}} e^{-0,5x^2}dx \qquad (10)$$

where: d – the permissible variability of μ_{cell}

It can be graphically shown as the field below the probability density of the normal distribution chart (Fig. 8).

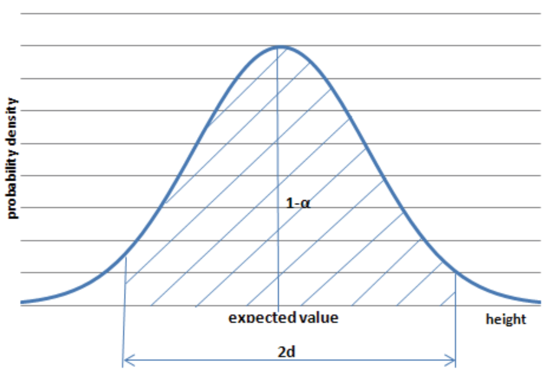

Fig. 8. Confidence level

Equation (10) may be also written with use of the distribution function F of the N(0,1) distribution:

$$1-\alpha = 2F\left(\frac{d\sqrt{n}}{2S_{cell}}\right) - 1 \qquad (11)$$

The confidence level calculated this way requires also calculating the standard deviation. It also does not take into consideration errors of each point coordinates evaluation by the laser scanner.

Due to these errors each point may belong to more than one cell and the probability that point belongs to the cell may be calculated geometrically (Fig. 9) according to equation:

$$p_{new} = \frac{A_{err \cap cell}}{A_{error}} \qquad (12)$$

where: p_{new} – probability of point belonging to the cell, A_{error} – total area of an error ellipsoid projected to the (x,y) plane, $A_{err \cap cell}$ – intersection area of an error ellipsoid projected to the (x,y) plane with the area of cell.

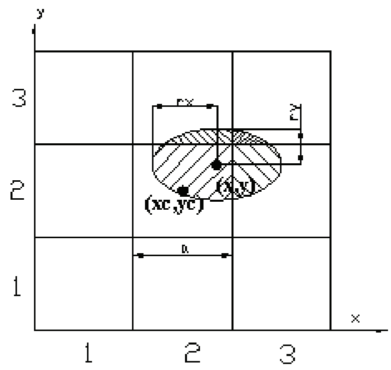

Fig. 9. The probability of belonging to the cell

Assumption that the point errors are an ellipsoid may be too complex due to $A_{err \cap cell}$ calculation problems. It may be easier to assume that the point errors are cuboid or cube.

Considering the point as a volume of points causes the need of modification of equation (5) to the form:

$$h_{cell\_new} = \frac{h_{cell} \cdot w + h_{new} \cdot w_{new}}{w + w_{new}} \qquad (13)$$

where: w – total weight of all points in the cell currently, w_{new} – weight of new point which is being added to the map in current step.

Proposed w_{new} calculation is based on r_x, r_y, r_z point errors and p_{new} probability of point belonging to the cell:

$$w_{new} = \frac{p_{new} \cdot a}{r_x r_y r_z} \qquad (14)$$

where: a – length of the side of each cell.

The cell dimension a which appears in equation (14) does not have an impact on the calculated average value but it has an impact on the value of confidence factor according to equation (15).

According to the requirements mentioned below a new confidence factor *CF* was proposed:

- CF has non-negative values, it increases when the information confidence becomes lower;
- CF decreases while increasing the number of points in the cell;
- when the number of points is big, adding a new point to the cell does not have a big impact at the CF factor.

Proposed equation for calculating the confidence factor was shown below:

$$CF = \frac{1}{\sum_{i=1}^{n} \frac{w_i}{{d_i}^2}} \qquad (15)$$

where: w_i – weight of the point, d_i – distance between the point height value and the current average height value in the cell (in the case when it is equal to zero, there is a need to evaluate d_i as a sufficiently small number to avoid dividing by zero).

When updating the map point-by-point another formula may be used:

$$CF_{new} = \frac{1}{\frac{1}{CF} + \frac{w_{new}}{{d_{new}}^2}} \qquad (16)$$

where: CF – confidence factor from previous step, CF_{new} – updated confidence factor, w_{new} – weight of new point, currently being added to the map, d_{new} – distance between new point height and updated average height.

Charts from Fig. 10 to Fig. 13 shows changes of confidence factor depending on changes of other elements of CF equation.

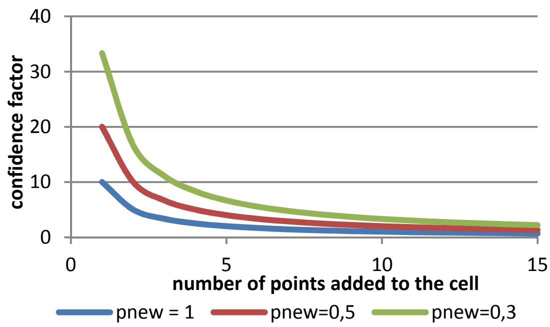

Fig. 10. Relation of confidence factor and number of points in the cell for different values of points probabilities (a, h_i, r_x, r_y, r_z where the same for each point)

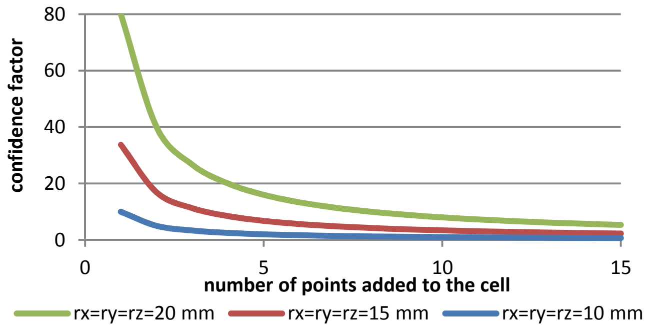

Fig. 11. Relation of confidence factor and number of points in the cell for different point errors values (a, h_i, p_i where the same for each point)

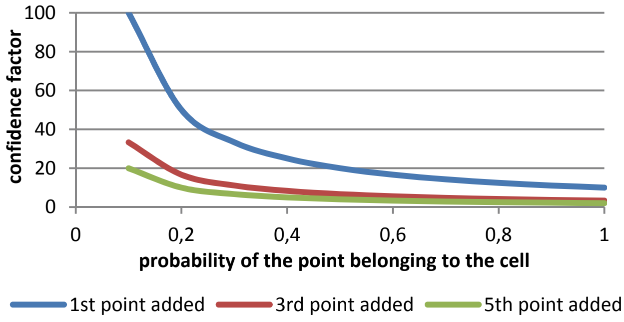

Fig. 12. Relation of confidence factor and probability of belonging to the cell for the same point added to the cell for the 1st, 3rd and 5th time (a, h_i, r_x, r_y, r_z where the same for each point)

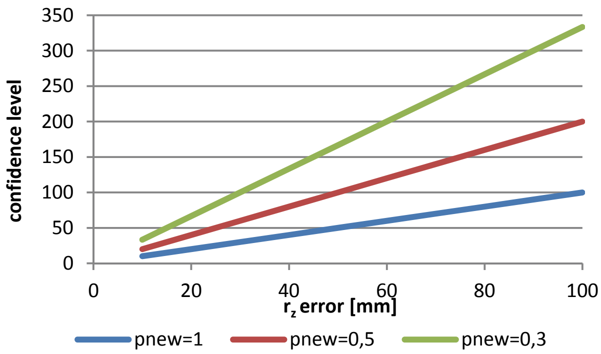

Fig. 13. Relation of confidence factor and r_z error of the point for different values of points probabilities (a, h_i, r_x, r_y where the same for each point).

6. Conclusions

In the 2,5D map used for description of the rough terrain for mobile robot navigation there is a problem of selecting appropriate parameters to describe height, slope, roughness and information confidence. As it was shown calculating height in each cell after adding new point to the map does not need large computational requirements (for each of selected parameters). For sure, the robot localization problem has an impact on the calculation time while adding a new point to the map from the laser scanner measurements. However it was out of scope of this paper. The main advantage of proposed solution of 2,5D map building was distinction of the height and slope description from the roughness description and the confidence level description.

Further research will focus on the path planning algorithms with use of the proposed 2,5D map and the development of proposed rough terrain description system.

AUTHOR

Adam Niewola – Technical University of Lodz, Institute of Machine Tools and Production Engineering, Stefanowskiego 1/15 St.; 90-924 Łódź; adam.niewola@gmail.com

References

[1] Tarutoko Y., Kobayashi K., Watanabe K., "Topological Map Generation based on Delaunay Triangulation for Mobile Robot". In: *SICE-ICASE International Joint Conference*, 2006, p. 492.

[2] Siemiątkowska B., Szklarski J., Gnatowski M., Zychewicz A., "Budowa hybrydowej semantyczno-rastrowej reprezentacji otoczenia robota", *Pomiary Automatyka Kontrola*, vol. 3, 2010, pp. 279–280 (in Polish).

[3] Ye C., JBorenstein J., "A Method for Mobile Robot Navigation on Rough Terrain". In: *International Conference on Robotics and Automation*, New Orleans 2004, pp. 3863–3865.

[4] Triebel R., Patrick Pfaff P., Burgard W., "Multi-Level Surface Maps for Outdoor Terrain Mapping and Loop Closing". In: *International Conference on Intelligent Robots and Systems*, Beijing, 2006, pp. 2276–2277.

[5] Fong E.H.L., Adams W., Crabbe F.L., Schultz A.C., "Representing a 3-D Environment with a 2,5-D Map Structure". In: *International Conference on Intelligent Robots and Systems*, Las Vegas, 2003, pp. 2987–2989.

[6] Podsędkowski L., Nowakowski J., Idzikowski M., Visvary I., "Modified A* algorithm suitable for on-line car-like mobile robots control", *Robot Motion and Control*, 1999, pp. 235–240.

[7] Podsędkowski L., Nowakowski J., Idzikowski M., Visvary I., "A new solution for path planning in partially known or unknown environment for nonholonomic mobile robots", *Robotics and Autonomous Systems*, vol. 34, issues 2–3, 2001, pp. 142–152.

[8] Porta Garcia M.A., Montiel O., Castillo O., Sepulveda R., Melin P., "Path planning for autonomous mobile robot navigation with ant colony optimization and fuzzy cost function evaluation", *Applied Soft Computing*, vol. 9, issue 3, 2009, pp. 1102–1110.

[9] Latombe J.-C., *Robot Motion Planning*, Kluwer Accademic Publishers, 1991, pp. 297–313.

[10] Tang L., Dian S., Gu G., Zhou K., Wang S., Feng X., "A novel Potential Field Method for Obstacle Avoidance and Path Planning of Mobile Robot", *IEEE International Conference on Computer Science and Information Technology*, vol. 9, 2010.

[11] Gu J., Cao Q., "Path planning using hybrid grid representation on rough terrain", *Industrial Robot: An International Journal*, vol. 36, no. 5, 2009, pp. 497–502.

[12] Bigaj P., "A memetic algorithm for global path planning with movement constraints for a nonholonomic mobile robot", PhD Dissertation, System Research Institute, Polish Academy of Sciences, publ. by PIAP, Warsaw 2012. ISBN: 978-83-61278-16-0.

[13] Amato N.M., Wu Y., "A Randomized Roadmap method for Path Planning and Manipulation Planning". In: *IEEE International Conference on Robotics and Automation*, 1996, pp. 113–120.

[14] Lingelbach F., "Path Planning of Mobile Manipulation using Probabilistic Cell Decomposition". In: *IEEE/RSJ International Conference on Intelligent Robots and Systems*, 2004, pp. 2807–2812.

[15] Podsędkowski L., Idzikowski M., "Robot localisation methods using the laser scanners". In: *4th International Workshop on Robot Motion and Control*, Puszczykowo, Poland, 2004, *Robot Motion and Control: Recent Developments*, 2006, vol. 335, pp. 315–332.

[16] Idzikowski M., Podsędkowski L., "Simulation and experimental results of a new method for mobile robot localization". In: *5th International Workshop on Robot Motion and Control*, Puszczykowo, Poland, 23rd–25th June 2005, pp. 175–179.